Available online at www.sciencedirect.com
ScienceDirect
International Journal of Coal Geology 71 (2007) 554–567
International Journal of COAL GEOLOGY
www.elsevier.com/locate/ijcoalgeo

Potential source rocks, organic geochemistry and thermal maturation in the southern depocenter (Kipourio–Grevena) of the Mesohellenic Basin, central Greece

P. Avramidis [*], A. Zelilidis

Department of Geology, University of Patras, 26500 Rio-Patras Greece

Received 8 February 2006; received in revised form 1 December 2006; accepted 11 December 2006
Available online 30 December 2006

Abstract

The study area is the southern depocenter (depth >4200 m) of the Mesohellenic Basin which extends between Kipourio and Grevena, central Greece. The Mesohellenic Basin is a Middle-Tertiary intramontane basin developed within the Hellenide orogen. Previous studies have focused on the depositional environments, configuration and hydrocarbon potential of the basin. In this paper we present additional geochemical and petrographic data from outcrop samples of the basin's southern depocenter, which is considered the most promising area, in terms of hydrocarbon prospectivity. A total number of thirty six samples were analysed: Rock-Eval pyrolysis, maceral analysis, vitrinite reflectance and thermal alteration index, bitumens extraction, liquid chromatography, and GC-MS. The samples were collected from deltaic deposits and submarine fan sediments of Late Eocene to Late Oligocene age. The TOC values of the analysed samples range between rich and very rich and the organic matter consists mainly of type III kerogen and the organic matter consider to be predominately gas prone. The thermal maturity assessed from T_{max} and vitrinite reflectance shows an immature stage of the organic matter along with the presence of layers having reached the very early mature stage. Vitrinite reflectance measurements and maturity calculations (applying the Lopatin modeling), reveal that the lower part of the depocenter sediments falls within the 'oil window'. The extractable organic matter (EOM) (mg bitumens/g TOC) indicate the existence of samples (from deltaic deposits) with high ratio of transformation (EOM) (>100 mg bitumen/g TOC). The GC and GC-MS analyses of the biomarkers indicate mainly the occurrence of terrestrial organic matter reflecting oxidizing conditions and both immature and very early mature stages. The results of the Rock-Eval pyrolysis and the distribution of the isoprenoids support the assumption of the input of an organic matter mixture.

Keywords: Hydrocarbon potential; Depositional environment; Organic geochemistry; Mesohellenic Basin, Greece

1. Introduction

The study area is the Mesohellenic Basin, a middle Tertiary intramontane basin, located in central Greece. It is 130 km long, and 40 km wide and trends SSE–NNW (Fig. 1a). The basin formed within the Hellenide orogen and developed from Late Eocene to Late Miocene time (Fig. 1b) as a piggy-back basin along the eastern flank of a giant pop-up structure (Robertson, 1994).

In the Mesohellenic Basin, hydrocarbon exploration activities have been carried out by the Public Petroleum Corporation of Greece, while studies dealing with analyses of depositional environments, basin configuration

---

[*] Corresponding author.
E-mail address: p.avramidis@upatras.gr (P. Avramidis).

doi:10.1016/j.coal.2006.12.006

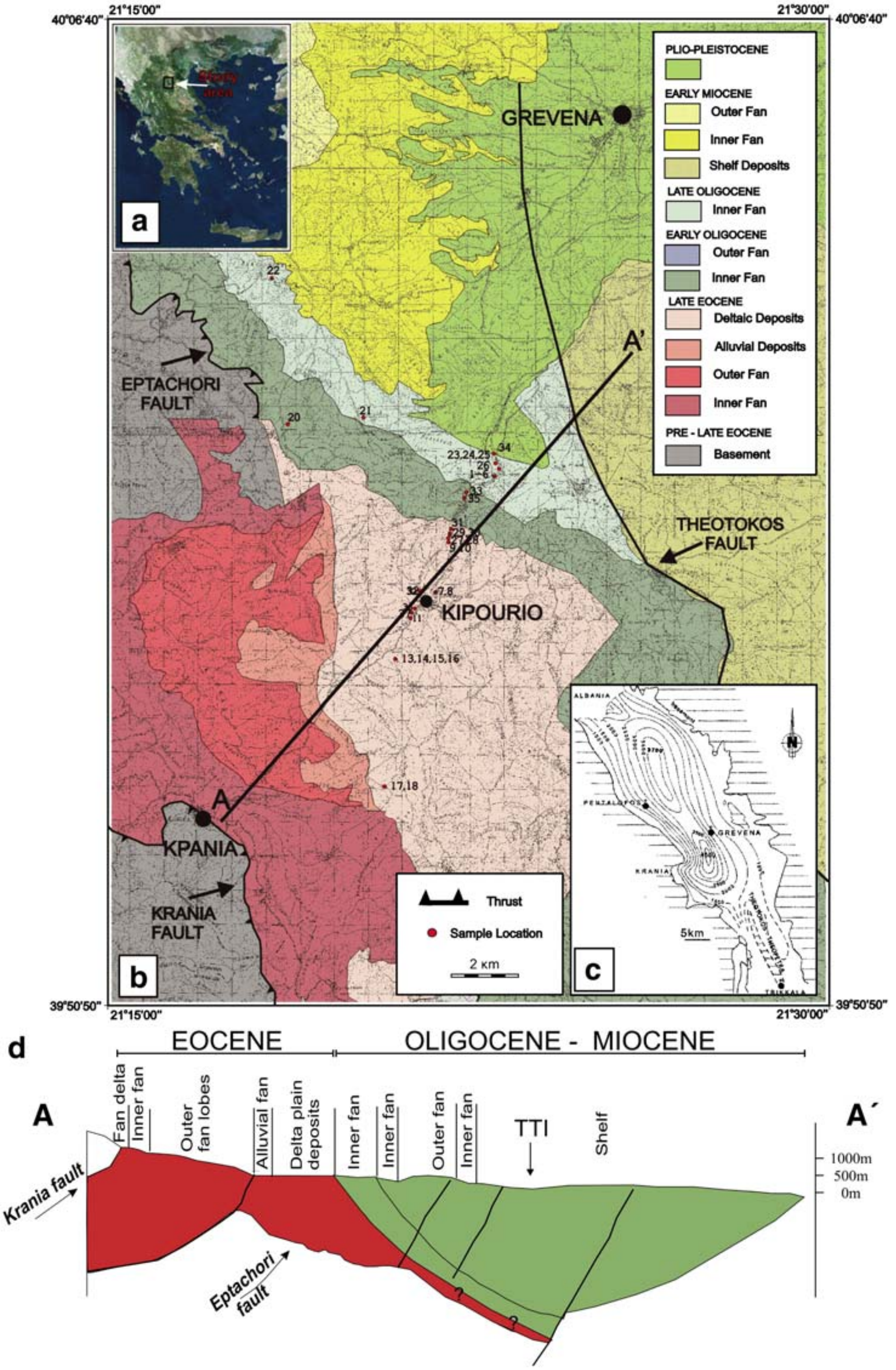

Fig. 1. a) Location of the study area, b) Geological map of the study area (Kipourio–Grevena); AA': the location of the cross-section (see Fig. 1d), c) Layout of the basin with isopach map showing the two depocenters and d) Geological cross-section modified from Kontopoulos et al. (1999) and Avramidis et al. (2002).

and the preliminary assessment of the hydrocarbon potential, have been reported by Kontopoulos et al. (1999), Avramidis et al. (2002) and Zelilidis et al. (2002). The basin comprises two depocentres, the first one in the northern part (>3200 m thick) and the second in the southern part (>4200 m thick) (Fig. 1c). The basin is filled with sediments of Late Eocene to Late Miocene age. The sedimentary sequences of the Mesohellenic Basin consist mainly of submarine fan (sandstone and shale) and deltaic deposits. The basin is considered to constitute a high-risk area in terms of hydrocarbon exploration (Avramidis et al., 2002); this is supported by the fact that up to now no commercial deposits have been discovered. A licensing round for hydrocarbon exploration and exploitation was held in 1996 (Roussos and Marnelis, 1995), while a second round will soon take place including areas in central and northern Greece, such as the Mesohellenic Basin (Mavromatidis et al., 2004).

The objective of the present paper is to present geochemical and petrographic data from outcrop samples from the southern hydrocarbon-prone depocenter of the basin.

2. Geological setting

The evolution of the Mesohellenic Basin was controlled by the activity of the Krania, Eptachori and Theotokos faults (Fig. 1b,d). During the Late Eocene, and due to the activity of the Krania thrust, fan deltas developed in the proximal part of the basin, and submarine fans in the distal part. Also during the Late Eocene, the Eptachori thrust was activated and fan deltas developed adjacent to the fault. Due to synchronous activity of these faults a structural platform formed, on which delta-plain sediments accumulated.

In early Oligocene times, only the Eptachori thrust was active and submarine fans developed throughout the basin. During Late Oligocene to Early Miocene, the subsidence of the Mesohellenic Basin varied as a result of differential thrust activity along the basin axis (Doutsos et al., 1994; Zelilidis et al., 1997). Due to varying tectonic regimes the basin evolved from a uniformly structured basin (Early Oligocene) to an internally partitioned basin (Late Oligocene–Early Miocene).

In the study area, mapping and interpretation of the depositional environments are based on sedimentological work by Zelilidis et al. (1997) and seismic investigation by Kontopoulos et al. (1999) (Fig. 1d), while a review of the geodynamic controls of the Mesohellenic Basin is given by Ferriere et al. (2004). Based on the studies covering the stratigraphy and the depositional environments, the basin evolution is interpreted – from the western to the eastern margin – as follows: a) Middle Eocene fan delta deposits, up to 100 m thick adjacent to the Krania fault, b) Middle to Late Eocene submarine fan deposits — inner fan showing a thickness of 600 m and outer fan 300 m, c) Late Eocene 900-m thick deltaic deposits, d) Early to Late Oligocene submarine fans, with a cumulative thickness of 1100 m comprising the inner and outer fan, and e) Miocene shelf sediments up to 900 m thick.

3. Materials and methods

Thirty-six samples (30 hand-picked from outcrops and 6 core samples) were studied in the Stratochem Laboratories using (a) Rock-Eval II pyrolysis (36 samples), (b) bitumen extraction, liquid chromatography and GC-MS (9 samples), and (c) maceral analysis and vitrinite reflectance measurements.

The basic geochemical and petrographic techniques applied, have been described in detail by Tissot and Welte (1984), Moldowan et al. (1985), Brooks et al. (1992), Killops and Killops (1993), Peters and Moldowan (1993), and Hunt (1996). In the present paper we followed the method of Espitalié et al. (1977) on the development and application of the Rock-Eval Pyrolyzer, and parameters such as TOC, T_{max}, Hydrogen Index (HI), Oxygen Index (OI), Productivity Index (PI) and S1, S2 and S3 were obtained.

Solvent extraction was carried out by soxhlet technique using chloroform and benzene/ethanol mixture (2:1). Asphaltenes were precipitated with hexane and the soluble fraction was separated into saturates, aromatics and resins (NSO compounds) on a silica-alumina column by successive elution using hexane, benzene, and benzene–methanol. The solvents were evaporated and the weight percent of each component was determined.

For the GC analysis, the sample of whole oil was injected directly into a Hewlett Packard 5890 Gas Chromatograph fitted with a Quadrex 50-meter fused silica capillary column. The GC was programmed from 40 to 340 °C at 10 °C/min with a 2-minute hold at 40 °C and a 20-minute hold at 340 °C. Analytical data were processed with a Nelson Analytical model 3000 chromatographic data system and an IBM computer hardware. All standard calculations were made including pristine/phytane ratio and carbon preference index. Two gas chromatograms were provided, one showing all compounds between nC2 and nC40 and the other a computer enhanced version of the chromatogram between nC2 and nC10. Compounds as low as ethane, could be detected if present. In addition, the concentration of C13 to C20 isoprenoids were determined and plotted.

Computerized Gas Chromatography/Mass Spectrometry (GC/MS) of saturate and aromatic fractions was used to evaluate various geochemical characteristics of oils and rock extracts, including organic facies, thermal maturity level and degree of alteration. The saturate and aromatic fractions were isolated by liquid chromatography from whole oils or source rock extracts and injected into a HP5890 Gas Chromatograph coupled to a HP5971A Mass Selective Detector (MSD). The analysis targeted two important hydrocarbon classes: triterpane and sterane biomarkers and 2- and 3-ring aromatic hydrocarbons. The Selected Ion Monitoring (SIM) feature of the GC/MS data acquisition system permits specific ions to be monitored. Ions with mass/charge (m/z) 191 allow characterization of specific triterpenoid compounds, while ions with m/z 217 are diagnostic for steranes. Steranes with different chemical structures can be identified using different ions. Thus, m/z 218 is characteristic of steranes with abb stereochemistry and diasteranes exhibit a pronounced m/z 259 fragment. In addition, molecular ions characteristic of individual triterpane and sterane compounds (m/z 370, 372, 384, 386, 398, 400, 412, 414 and 426) are acquired. These molecular ions are not provided as part of the routine analytical report, but are available to confirm peak identifications and to identify unknown compounds. In addition to saturated steranes, monoaromatic and triaromatic steranes were identified in the aromatic fractions by the ions m/z 253 and 231, respectively.

A Zeiss Universal microscope system was used for maceral analysis. Maceral analysis was performed in 15 samples, either in whole sample or after acid treatment, using reflected and transmitted light and blue-light excitation. The nomenclature applied in the analysis was based, in general, on the classification described by Stach et al. (1982). For the texture of the unstructured lipids the terminology proposed by Castaòo and Sparks (1974) and Potter et al. (1998) was followed; according to this, the various types of vitrinite were grouped into one group unless it could be identified as ‘lipid-rich (or hydrogen-rich) vitrinite’ (Lo, 1993). Noteworthy to mention that in this study the term ‘vitrinite’ also includes humic components of low rank (i.e. huminite).

The vitrinite reflectance measurements were performed on a polished block in reflected light and TAI was performed on a strewn slide in transmitted light. A halogen light source was used for vitrinite reflectance with a digital indicator calibrated against a glass standard with a reflectance of 1.02% in oil immersion ($n_d = 1.516$ at 23 °C). This calibration is linearly accurate for reflectance values ranging from peat (0.20% Ro) through anthracite (4.0% Ro). A xenon light source was applied for blue-light excitation using a filter at 495 nm, a barrier filter at 520 nm and a tungsten light source for TAI analysis. The purpose of the analysis was to measure thermal maturation rather than exact identification of macerals.

4. Results and discussion

The location and the depositional environment for each sample are presented in Fig. 1b, while their coordinates and Rock-Eval results are showed in Table 1. The organic geochemistry results, as well as the maceral analysis, the vitrinite reflectance and the TAI are presented on Table 2.

4.1. Rock-Eval pyrolysis

The TOC contents of five outer-fan (Late Oligocene) samples representing lignite intercalations, vary from 27.58% and 56.24% (Table 1). The genetic potential ($S_1 + S_2$) of these samples ranges from 28.43 to 66.07 kg HC/t rock and given the type of kerogen (Table 1), it indicates a potential for gas generation. The respective hydrogen index (HI = S2/TOC) vs. oxygen index (OI = S3/TOC) plot on the van Krevelen diagram (van Krevelen, 1984; Tissot and Welte, 1984), indicates the predominance of organic matter of type III (Fig. 2a). The T_{max} values range from 410 to 432 revealing an immature to very early mature level (Table 1; Fig. 3). The S2/S3 ratio (Peters, 1986), in combination with the types of the organic matter, indicates that the potential of these sediments is to produce mainly gas ($S2/S3 < 2$) with exception of samples #23 and #26, where $S2/S3 > 5$, while PI values range from 0.06 to 0.1 (Table 1).

The eleven inner fan (Middle–Late Oligocene) samples are characterised by types III and IV kerogen (Fig. 2b). Although there are samples with high genetic potential (samples #1, 35, 5, 6, 12, 22, 33), the HI being < 100 and the relatively low T_{max} values (< 430) indicate that the organic matter is thermally immature (Table 1; Fig. 3). The S2/S3 ratio in relation to the kerogen type indicates basically a limited ability for gas generation and only sample #12 (with higher HI) may has a minor potential for liquid hydrocarbons generation. Noteworthy, the PI values of three samples (#2, 6 and 21) are relatively high (Table 1).

The two inner fan (Early Oligocene) samples are projected as kerogen types III and IV, in the HI vs. OI diagrams (Table 1; Fig. 2c). Although the genetic

Table 1
Rock-Eval pyrolysis data

SAMPLE	Long/Lat	TOC	S1	S2	S3	T_{max}	HI	OI	PI	S2/S3	PP
Upper Oligocene — outer fan deposits											
23	39°59′67″N 21°23′05″E	31.57	3.73	62.34	6.85	411	197	22	0.06	9.10	66.07
24	39°59′46″N 21°23′31″E	38.16	0.9	27.53	9.44	424	72	25	0.03	2.92	28.43
25	39°59′46″N 21°23′31″E	51.47	1.09	37.92	8.75	418	74	17	0.03	4.33	39.01
26	39°59′46″N 21°23′31″E	27.58	4.51	40.28	5.41	410	146	20	0.1	7.45	44.79
34	39°59′37″N 21°23′22″E	56.24	0.5	33.69	9.58	432	60	17	0.01	3.52	34.19
Middle–upper Oligocene — inner fan deposits											
1	39°59′37″ N 21°23′22″E	5.41	0.35	5.56	1.31	425	103	24	0.06	4.24	5.91
2	–//–	0.71	0.19	0.42	0.38	314	59	54	0.31	1.11	0.61
3	–//–	4.43	0.14	2.8	1.15	387	63	26	0.05	2.43	2.94
4	–//–	3.89	0.21	3.67	1.19	374	94	31	0.05	3.08	3.88
5	–//–	15.06	0.48	11.02	2.4	420	73	16	0.04	4.59	11.5
6	–//–	8.78	2.42	13.3	1.68	396	151	19	0.15	7.92	15.72
12	39°59′23″N 21°23′03″E	42.72	1.4	103.47	7.02	406	242	16	0.01	14.74	104.87
21	30°00′34″N 21°20′11″E	12.83	0.31	1.63	7.63	328	13	59	0.16	0.21	1.94
22	40°02′37″N 21°18′52″E	53.23	2.12	52.55	9.16	417	99	17	0.04	5.74	54.67
33	39°58′85″N 21°22′41″E	51.97	0.74	26.33	12.91	436	51	25	0.03	2.04	27.07
35	39°57′35″N 21°22′44″E	38.66	0.44	9.92	13.25	360	26	34	0.04	0.75	10.36
Lower Oligocene — inner fan deposits											
20	39°58′31″N 21°22′12″E	8.16	0.59	2.13	5.55	439	26	68	0.22	0.38	2.72
31	40°00′12″N 21°18′61″E	48.26	1.18	54.61	9.08	428	113	19	0.02	6.01	55.79
Upper Eocene — deltaic deposits											
7	39°58′20″N 21°02′10″E	54.9	15.28	137.92	13.43	409	251	24	0.1	10.27	153.2
8	39°58′20″N 21°02′10″E	14.52	0.3	11	5.98	423	76	41	0.03	1.84	11.3
9	39°58.11″N 21°22′10″E	55.6	5.47	146.28	12.51	417	263	23	0.04	11.69	151.75
10	39°58′11″N 21°22′10″E	56.12	0.72	35.95	12.45	440	64	22	0.02	2.89	36.67
11	39°58′02″N 21°22′08″E	55.01	0.35	25.65	12.11	459	47	22	0.01	2.12	26
13	39°58′02″N 21°22′08″E	57.48	2.53	36.06	13.36	427	63	23	0.07	2.70	38.59
14	39°57′77″N 21°22′05″E	65.73	43.08	163.33	3.94	391	248	6	0.21	41.45	206.41
15	39°58′72″N 21°22′44″E	64.94	40.31	172.29	3.2	387	265	5	0.19	53.84	212.6
16	39°57′24″N 21°21′25″E	67.31	44.24	213.17	3.33	385	317	5	0.17	64.02	257.41
17	39°59′24″N 21°23′25″E	5.23	0.48	10.14	0.45	422	194	9	0.05	22.53	10.62
18	39°56′89″N 21°22′23″E	35	3.82	120.98	1.62	407	346	5	0.03	74.68	124.8
27	39°56′76″N 21°21′08″E	54.56	0.45	22.31	11.35	452	41	21	0.02	1.97	22.76
28	Boreholes	45.24	3.4	111.81	13.53	416	247	30	0.03	8.26	115.21
29	–//–	44.61	0.4	22.87	11.49	435	51	26	0.02	1.99	23.27
30	–//–	59.23	5.36	159.46	12.45	417	269	21	0.03	12.81	164.82
32	–//–	61.78	12.2	136.16	9.3	411	220	15	0.08	14.64	148.36
36	–//–	56.38	0.77	30.13	12.23	438	53	22	0.02	2.46	30.9
37	–//–	44.82	0.56	23.88	11.66	433	53	26	0.02	2.05	24.44

potential seems to be moderate to high, the low HI values (<115) and the kerogen types, infer that the results are obviously not unequivocal.

The eighteen deltaic (Late Eocene) samples indicate the presence of source rocks differing from the above examined layers, by indicating kerogen type II (samples #7, 9, 14, 14,15, 16, 17, 18, 28, 30 and 32) and type III (#8, 10, 11, 13, 27, 29, 36 and 37). The PIs (0.17–0.21) indicate mature levels for samples #14, 15, 16, and immature levels for the remainder samples (Fig. 1; Table 1). All analysed samples from the deltaic deposits have a high genetic potential ranging from 10.62 to 257.41 kg HC/t rock. Almost all the examined samples are characterised by a S2/23>5 showing the existence of layers which could produce liquid hydrocarbons. Exceptions are samples #8, 27, and 29. Moreover, based on T_{max} results, layers have been identified, which show readings (T_{max} >425) pertaining to the ‘oil window’ but the low HI shows a minor hydrocarbon potential (Fig. 3).

Table 2
Organic geochemistry — petrology results of the studied samples

	EOM	Vitrinite reflectance				Fractionation of Extracts L.C.					Isoprenoids			Triterpanes	Steranes			Organic matter				T.A.I.
Sample	mg/g	Min	Max	STDEV	R0	Saturates	Aromatics	NSO	Asphaltenes	Pr/ Ph	Pr/ nC17	Ph/ nC18	OEP	Ts/Tm	C27	C28	C29	Lipids	Humic		Other	Color/ intense
																			Inertinite	Vitrinite		
Outer fan — Late Oligocene																						
24	–	0.41	0.55	0.04	0.48	–	–	–	–	–	–	–	–	–	–	–	–	5	–	–	95 (lipid rich vitrinite)	Yellow/ 2
34	1.54				0.57	5.30	4.90	57.10	32.70	0.20	0.60	5.50	1.11	0.98	0.04	0.11	0.85	30	–	–	70 (lipid rich vitrinite)	–
Inner fan — middle Late Oligocene																						
22	55.75	0.47	0.57	0.02	0.53	2.00	6.80	22.10	69.20	2.20	1.10	1.30	1.52	0.22	0.17	0.17	0.61	–	–	100	–	Yellow– orange/2
35	–				0.42	–	–	–	–	–	–	–	–	–	–	–	–	25	–	75	–	Yellow– orange/1
Inner fan — Early Oligocene																						
31	–	0.48	0.55	0.02	0.52	–	–	–	–	–	–	–	–		–	–	–	–	–	–	100	–
Deltaic deposits — Late Eocene																						
7	95.68	0.27	0.35	0.02	0.32	–	–	–	–	–	–	–	–	–	–	–	–	70	–	30	–	Orange/ 1
10	–	0.43	0.54	0.03	0.48	–	–	–	–	–	–	–	–	–	–	–	–	–	–	0	100 (lipid rich vitrinite)	–
11	–	0.42	0.54	0.02	0.48	–	–	–	–	–	–	–	–	–	–	–	–	–	–	50	50 (lipid rich vitrinite)	–
14	156.66	0.44	0.52	0.03	0.48	0.50	1.90	33.10	64.60	0.80	0.70	0.60	–	–	–	–	–	10	–	90	–	Orange– yellow/4
15	159.04	0.43	0.52	0.02	0.48	–	–	–	–	–	–	–	–	–	–	–	–	20	–	80	–	Yellow/ 4
16	–	0.44	0.50	0.02	0.48	–	–	–	–	–	–	–	–	–	–	–	–	30	–	70	–	Yellow/ 4
18	62.82	0.36	0.56	0.06	0.48	1.60	9.80	42.30	46.30	1.00	1.90	2.80	1.67	0.77	0.12	0.13	0.75	–	–	60	40 (lipid rich vitrinite)	Yellow/ 2
27	8.47	0.48	0.58	0.03	0.52	3.90	6.00	75.80	14.30	0.60	1.00	1.80	0.70	0.40	0.08	0.14	0.76	–	–	–	100 (lipid rich vitrinite)	Orange/ 2
29	5.60	0.44	0.51	0.02	0.48	–	–	–	–	–	–	–	–	–	–	–	–	–	–	–	100 (lipid rich vitrinite)	–
37	11.52	0.47	0.59	0.03	0.53	3.00	5.80	42.40	48.80	1.20	0.90	0.90	1.37	0.30	0.05	0.10	0.84	–	–	10	90 (lipid rich vitrinite)	Orange/ 2

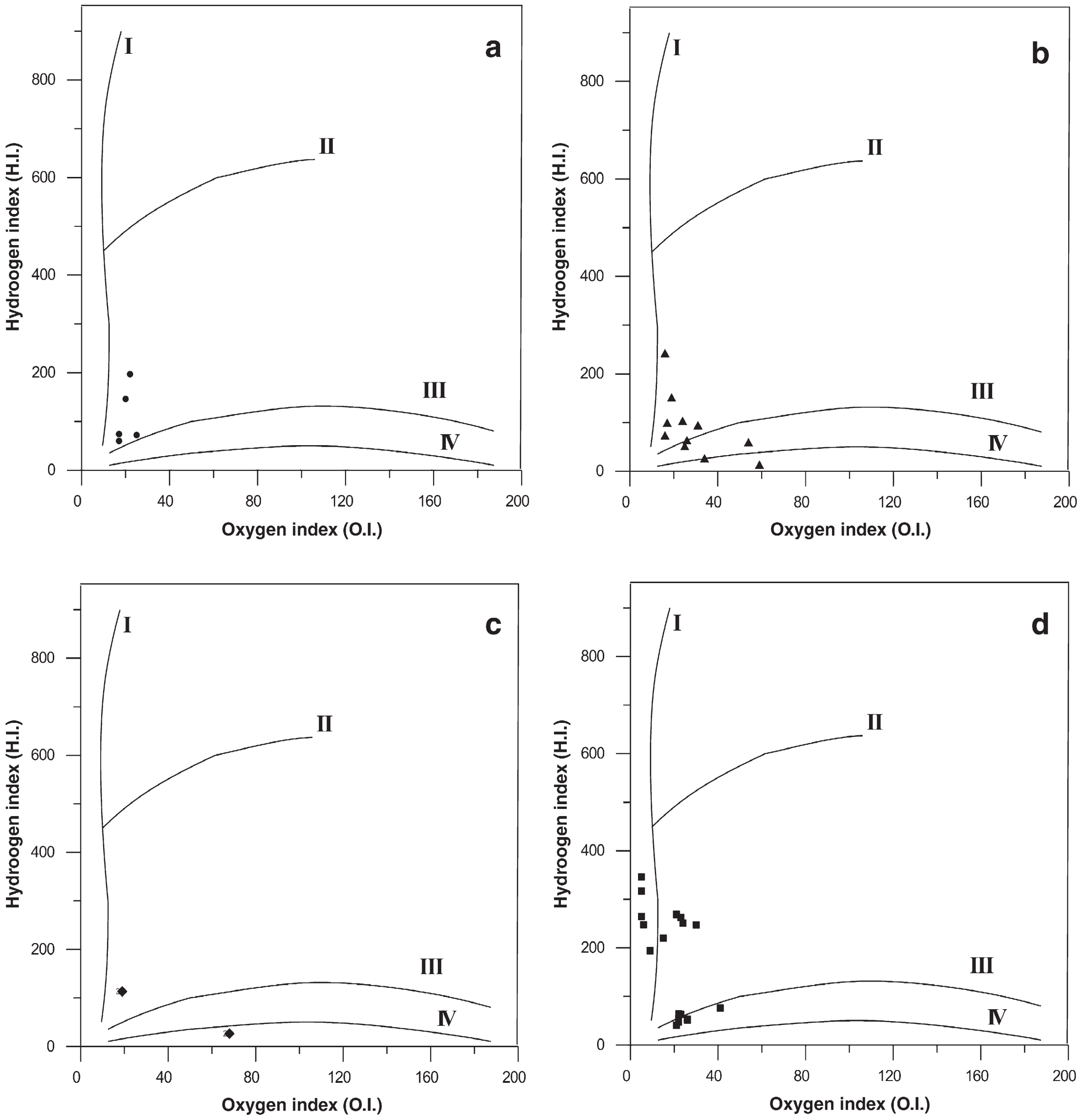

Fig. 2. Plot of HI *versus* OI for the analysed samples from the (a) Late Oligocene-outer fan deposits, (b) Middle to Late Oligocene inner fan deposits, (c) Early Oligocene inner fan deposits and (d) Late Eocene deltaic deposits.

4.2. Extractable organic matter — LC-GC-GCMS

The EOM (mg/g rock) calculated from bitumen extraction using Soxhlet apparatus, is used as a maturity indicator. The yield of the deltaic samples >150 mg/g (Table 2), is higher than this obtained from the Oligocene submarine fan. This may indicate migrated hydrocarbons (Tissot and Welte, 1984) and the respective level of maturity. Although we have high ratio of EOM mg/g rock, the extract composition reveals the dominance of NSO compounds, which is in agreement with the immature or the very early mature stage (Tissot and Welte, 1984) (Fig. 4; Table 2).

The GC analysis (Fig. 5) can also be used for interpretation of environmental conditions at the time of deposition and the source of the organic matter (Tissot and Welte, 1984; Moldowan et al., 1985; Killops and Killops, 1993; Hunt, 1996). The relative abundance of the isoprenoids pristane to phytane and pristane/n-C17 to phytane/n-C18 represents different environmental conditions (Dydik et al., 1978; Leythaeuser and Schwarzkopf, 1986; see Fig. 6). The pr/ph ratio ranges

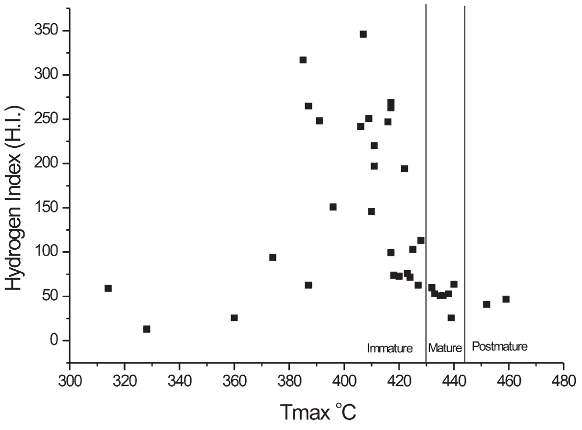

Fig. 3. HI *versus* T_{max} diagram for the examined samples.

between 0.2 and 2.2, indicating both oxidizing (#22 and 37) and reducing conditions (samples #27, 34 and 14; see Table 2). The respective plot on the pr/n-C17 and ph/n-C18 diagram indicates mainly oxidizing conditions and terrestrial input of organic matter.

The GC-MS analysis of the saturated fractions (Fig. 7) and the triterpane Ts/Tm ratio show early to mature levels of maturity ranging from 0.30 to 0.98 (Table 2). Samples #22, 27 and 37 are at the early mature stage, while #14, 18 and 34 are at the mature stage. The distribution of the normal steranes and the respective C27– C28– C29 ternary diagram (Fig. 8), show a possible source from siltstones containing lignite lenses (samples #19, 27, 37, 34; see Table 2). Huang and Meinschein (1978) proposed that the distribution of C27 through C29 steranes in oils and rock extracts can be used as an indicator of biological origin and depositional environment. They suggest that C27 steranes derive from plankton, whereas C29 steranes derive from terrestrial sources such as higher land plants. The analysed samples are characterized by the dominance of C29 sterane and thus, are interpreted to indicate a terrestrial origin of the organic matter (Fig. 8) (MacKenzie et al., 1982).

4.3. Maceral analysis — Vitrinite reflectance–TAI

4.3.1. Late Oligocene outer fan samples

Sample #24: Most vitrinite fragments are lipid-rich with cell-structure remnants, which lower the reflectance (0.48%), holes, slits, etc. There are some large fragments of root or bark tissue with suberinite. Both the woody parts and the root or bark portions of plants are present. Maturity is at the top of the oil generation zone.

Sample #34: Organic matter consists of oxidized, lipid-rich vitrinite and unstructured material (Fig. 9d)

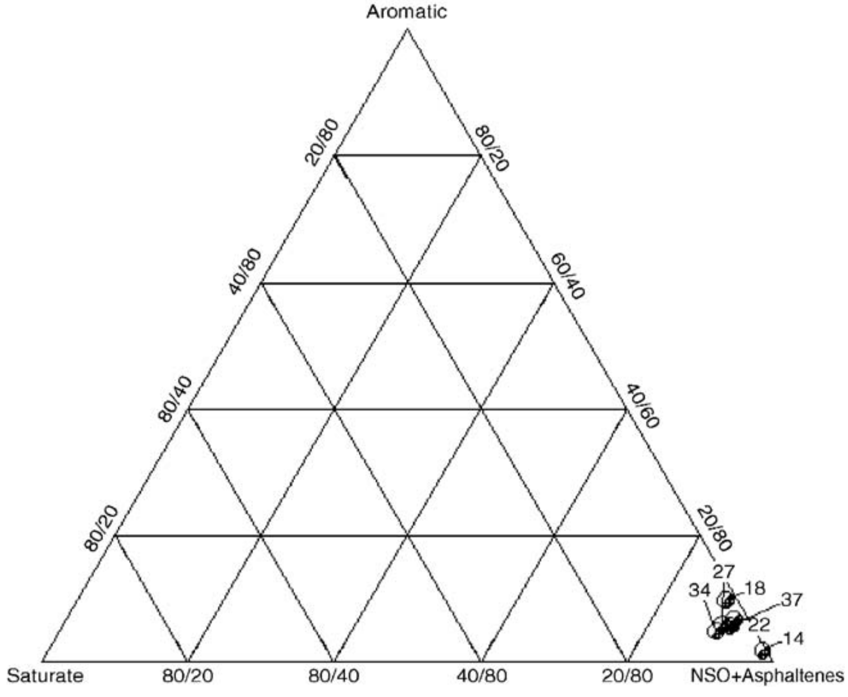

Fig. 4. The EOM composition of the studied samples.

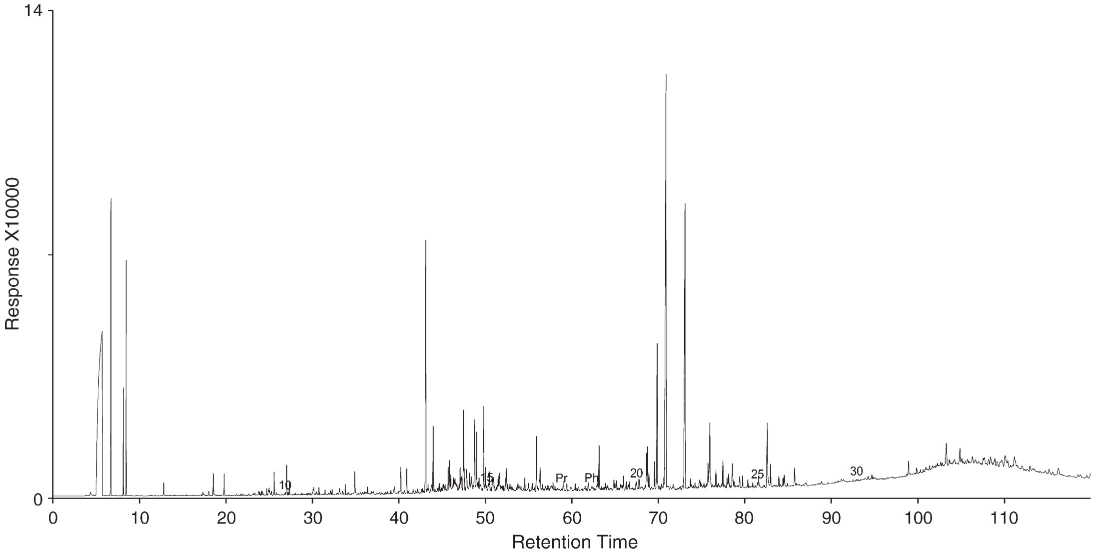

Fig. 5. The gas chromatography diagram for the deltaic sample #18.

that may be degraded humic debris. Some reflectance values (0.57%) may be lowered by oxidation. The pyrolysis data, however, indicate that maturity is at a very early mature stage. Degraded humic debris indicates that the unstructured material is probably from terrestrial sources. Humic debris means small, low-rank terrestrial fragments that cannot be identified.

4.3.2. Middle-Late Oligocene inner fan samples

Sample #22: Organic matter consists of large vitrinite fragments with some exsudatinite in fractures and some liptodetrinite inclusions. Vitrinite may be slightly lipid-rich. Vitrinite reflectance (0.53%) indicates that the organic matter is immature or may be at the very top of the oil window. Rock-Eval T_{max} may be slightly lowered by exsudatinite.

Sample #35: Coal fragments consist of compressed vitrinite components with abundant resin bodies. Fragments exhibit cell structure that is different from the remnant cell structure of lipid-rich vitrinite. Vitrinite reflectance (0.42%) and pyrolysis data indicate that the organic material is immature for oil generation. Resinite may lower the pyrolysis T_{max} value.

4.3.3. Early Oligocene inner fan samples

Sample #31: Vitrinite reveals characteristics of slightly lipid-rich vitrinite (Fig. 9c) as in sample #29, but reflectance values do not appear to be lowered. The vitrinite reflectance (0.52%) and the pyrolysis data indicate that maturity is in the oil generation zone.

4.3.4. Late Eocene deltaic samples

Sample #7: The organic matter consists of moderately oxidized lignite fragments, angular exsudatinite or solid bitumen with orange fluorescence, and unstructured material in a mineral groundmass. Some coals may form exsudates at the lignite/sub-bituminous coal boundary during coalification. Algae, animal plankton, fats and waxes experience anaerobic saprofication during which fatty acids and other substances form.

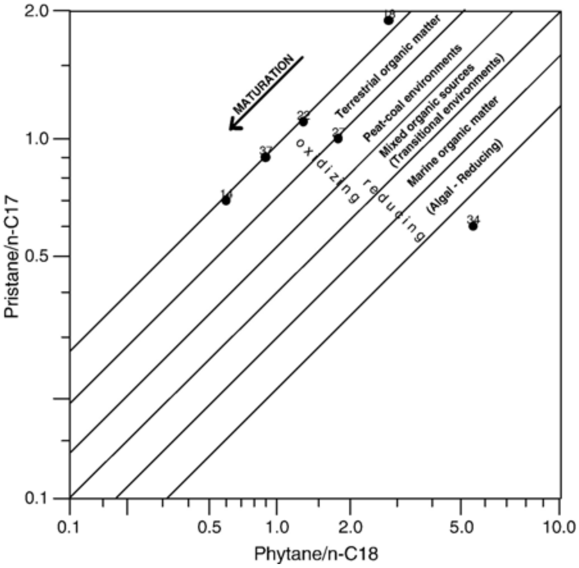

Fig. 6. Plot of pristane/n-C17 *versus* phytane/n-C18 showing the origin of the organic matter (fields after Hunt, 1996).

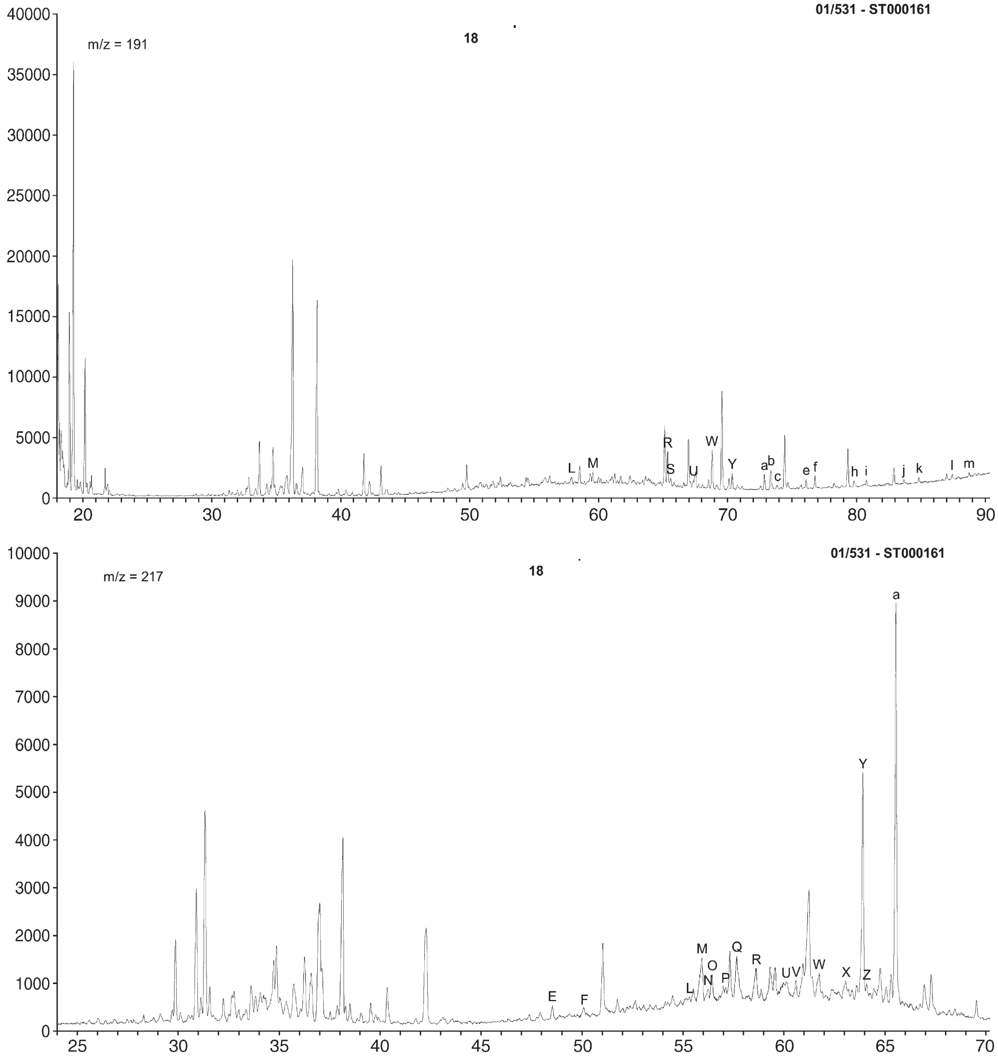

Fig. 7. Representative triterpanes (m/z of 191) and steranes (m/z 217) for fragmentation for sample #18 (deltaic deposit).

The vitrinite reflectance (0.32%) and the pyrolysis data indicate that the organic matter is immature for oil generation.

Sample #10: The organic matter consists of large, slightly lipid-rich vitrinite fragments. Vitrinite exhibits remnant cell structure, holes, characteristic fractures, and some oily (exsudanite, bituminite) spots, but it does not fluoresce. The reflectance values (0.48%) may be slightly lowered by the lipid content and reveal that maturity is probably at the top of the oil generation zone, although pyrolysis data show a maturity in the mid oil generation zone.

Sample #11: Some vitrinite fragments appear to be normal and some are similar to the lipid-rich vitrinite in sample #10, but without cell structure remnants. Some reflectance values may be slightly lowered by the lipids contained. The reflectance (0.48%) indicates that maturity is at the top of the oil window, but pyrolysis data indicate that maturity is in the lower oil generation zone.

Samples #14, 15, 16: The organic matter consists primarily of large telinite (cell wall) fragments with resinite or other lipid cell filling (Fig. 9a, b). Some large, normal vitrinite (Type A) fragments are also present. Vitrinite reflectance (0.48%) shows that maturity is approaching the top of the oil window. Pyrolysis T_{max} may be lowered by the large amount of resinite.

Sample #18: Large coal fragments have been observed, with some yellow fluorescing exsudatinite

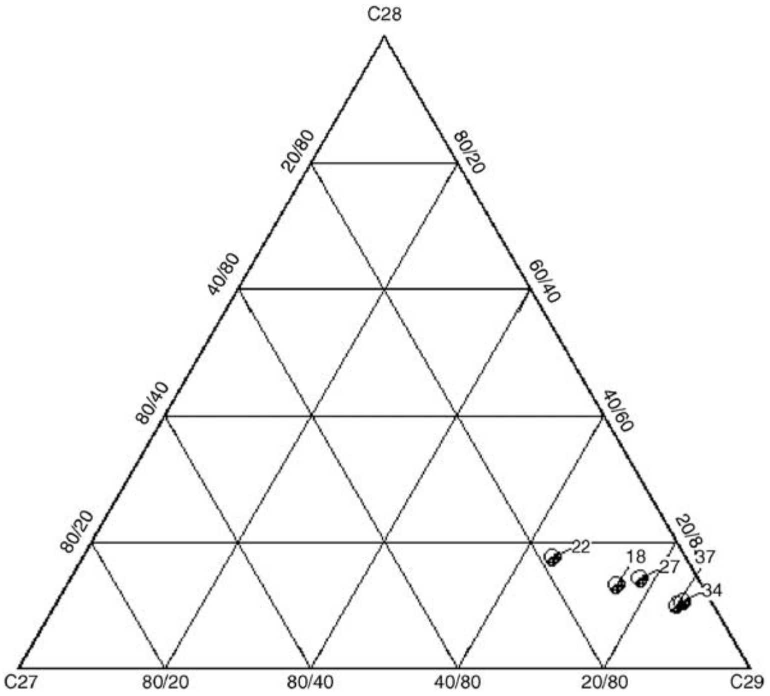

Fig. 8. Ternary diagram showing the relative abundance of C27–C28–C29 normal steranes.

in fractures. Some fragments appear normal and some are lipid-rich with remnant cell structure and lowered reflectance. The reflectance (0.48%) indicates that maturity is approaching the top of the oil generation zone. Pyrolysis T_{max} may be lowered by exsudatinite.

Sample #27: All vitrinite fragments are lipid-rich with cell structure remnant, slits, fractures, etc. Reflectance values may be slightly lowered. The reflectance (0.48%) shows that maturity is in the upper oil generation zone, but pyrolysis data indicate that maturity is in the mid oil generation zone.

Sample #29: Vitrinite is slightly lipid-rich with remnant cell structure, slits, oily spots, etc., and vitrinite reflectance values (0.48%) may be slightly lowered. Pyrolysis data indicate that maturity is in the oil generation zone.

Sample #37: The vitrinite reveals characteristics of slightly lipid-rich vitrinite — some oily spots, holes, faint remnant of cell structures and some slits. Oily spots occur when oily components in the lipid-rich vitrinite leak to the surface of the vitrinite after polishing. Reflectance (0.53%) and pyrolysis data indicate that maturity is in the oil generation zone.

Thermal Alteration Indices (TAI, see Table 2) based on colour intensity, show a mature level (Staplin, 1969), only for samples from the Late Eocene deltaic deposits (samples #14, 15, 16), while the presence mostly of vitrinite suggests a terrestrial origin of the organic matter (Teichmueller, 1986). The results of the analysis are similar and in agreement to those of Gerolymatos et al. (1988).

4.4. Burial history — TTI

In order to estimate the theoretical maturity of the organic matter, we used the Lopatin Time–Temperature Index method, adapted by Waples (1980). The TTI was calculated for a location in the central and deepest part of the Basin (Fig. 1d). Concerning the lack of boreholes and taking into account the sedimentary records from outcrops and seismic profile (Kontopoulos et al., 1999), in the calculation of TTI we used a geothermal gradient of 25 °C/km (Fig. 10), as a conservative approach for the study area. The burial history is based on depositional environments and basin evolution models of Kontopoulos et al. (1999) and Avramidis et al. (2002). The age determination based on the contained nannofossils, studied by Stoykova et al. (2002). Isopachs data for the clastic sediments, overlying the ophiolitic basement, were obtained from the seismic interpretations after Kontopoulos et al. (1999).

The TTI calculation, based on the geological model and age determinations, indicates that hydrocarbon generation could only be expected in the lower part of

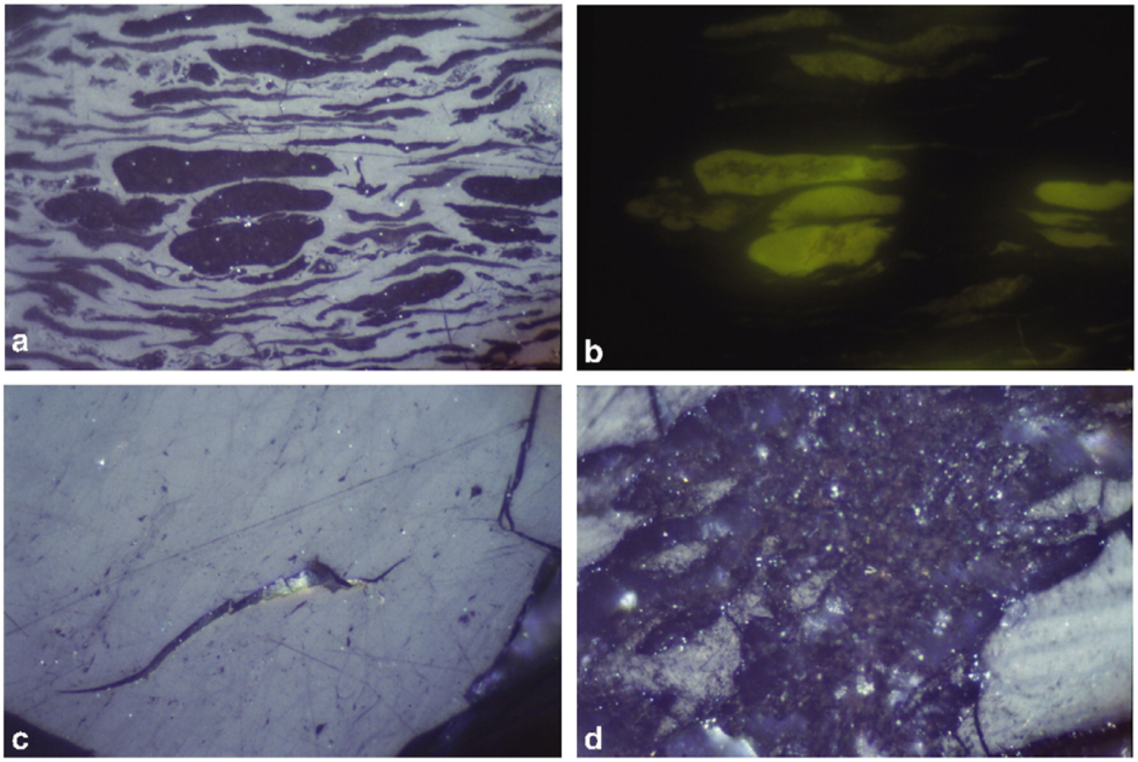

Fig. 9. Representative photos showing (a) telinite with resinite and cell filling in plane light and (b) in fluorescent light, from sample #14, representing late Eocene deltaic deposits. (c) slightly lipid-rich vitrinite in plane light, from sample #31, representing Early Oligocene inner fan deposits, and (d) lipid-rich vitrinite and unstructured debris in plane light, from sample #34, representing Late Oligocene inner fan deposits.

the late Eocene deltaic sediments, which are modeled to be within the top oil-window (early mature level) (Fig. 10).

5. Conclusions

Sediments sampled from outcrops and cores from the Mesohellenic Basin, central Greece, indicate a fluctuation of the organic matter content from rich to very rich, the occurrence of different source material, the different sedimentary environments and the early maturation stage of organic matter. These different features across the basin are related to the clastic sedimentation of the sub-marine fan and deltaic deposits; their mineralogical and chemical components are mainly affected by the mode and the agent of transport. From the geochemical and petrographic analyses of the outcrop samples we can infer that the main feature of the organic matter is the thermal immaturity and the existence of limited potential source rocks, having reached the very early stage of ‘oil maturity’. From the TTI model it seems that the deepest part of the southern depocenter (deltaic deposits) can be thermally mature. Up to now, however, the area has to be considered as a high-risk area for hydrocarbon exploration, and additional geochemical work has to be performed for the purpose of calibrating all the maturity data with deep borehole data. The analytical geochemical work carried out, as well as the burial history (described from TTI calculation) show that the only potential mature source rocks are included within the Upper

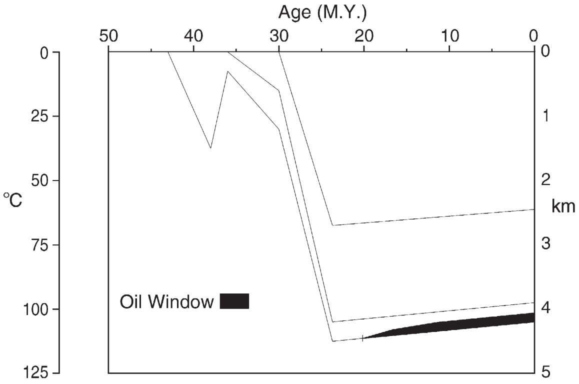

Fig. 10. TTI modeling of Lopatin method, after Waples (1980). Location: at the deepest part of the basin (Fig. 1d).

Eocene deltaic deposits. These deposits rendered indications of the presence of mature, hydrocarbon - prone layers.

The type of organic matter is related to the sediment charge of the Basin derived from different sources. The organic material of the submarine fans and the deltaic sediments derived mainly from terrestrial depositional environments that were eroded and carried towards the deeper parts of the Basin, *via* a delta system and submarine canyons. The organic matter includes mainly kerogen type III for the submarine fan deposits and types II and III for the deltaic deposits. The organic matter is predominately gas prone; both the thermal maturity assessed from T_{max} and the vitrinite reflectance indicate that the organic matter is thermally immature to early mature. The results of the Rock-Eval pyrolysis and the biomarkers distribution support the assumption of the input of an organic matter mixture. Integration of all geochemical–petrographic analyses and TTI data indicate that the lower part of the deltaic deposits has a possible hydrocarbon potential and should attract the main interest for further research.

Acknowledgements

This study was carried out at the Department of Geology, University of Patras, during a scholarship tenure of the first author from the Greek State Scholarship's Foundation (I.K.Y.).

Appendix A

Identification of peaks for sample #18 from deltaic deposits (see Fig. 7).

TRITERPANE REPORT (m/z 191)

Sample No. ST000161 Other ID: 18

No.	ID	Triterpane name	Ret time	Area	Area %	PPM
1	A	C_{19} Tricyclic Terpane		0	0.00	<1
2	B	C_{20} Tricyclic Terpane		0	0.00	<1
3	C	C_{21} Tricyclic Terpane		0	0.00	<1
4	D	C_{22} Tricyclic Terpane		0	0.00	<1
5	E	C_{23} Tricyclic Terpane		0	0.00	<1
6	F	C_{24} Tricyclic Terpane		0	0.00	<1
7	G	C_{25} Tricyclic Terpane (22R)		0	0.00	<1
8	G	C_{25} Tricyclic Terpane (22S)		0	0.00	<1
9	H	C_{24} Tetracyclic Terpane		0	0.00	<1
10	I	C_{26} Tricyclic Terpane (22R)		0	0.00	<1
11	I	C_{26} Tricyclic Terpane (22S)		0	0.00	<1
12	J	C_{28} Tricyclic Terpane (22R)		0	0.00	<1
13	J	C_{28} Tricyclic Terpane (22S)		0	0.00	<1
14	K	C_{29} Tricyclic Terpane (22R)		0	0.00	<1
15	K	C_{29} Tricyclic Terpane (22S)		0	0.00	<1
16	L	C_{27} 18aH-Trisnorhopane (Ts)	57.711	4587	3.96	23
17	M	C_{27} 17aH-Trisnorhopane (Tm)	59.367	5969	5.15	30
18	N	C_{30} Tricyclic Terpane (22R)		0	0.00	<1
19	N	C_{30} Tricyclic Terpane (22S)		0	0.00	<1
20	O	C_{28} 17aH, 18aH, 21bH-28, 30-Bisnorhopane		0	0.00	<1
21	P	C_{31} Tricyclic Terpane (22R)		0	0.00	<1
22	Q	C_{29} 17aH, 21bH 25-Norhopane		0	0.00	<1
23	P	C_{31} Tricyclic Terpane (22S)	65.121	0	0.00	<1
24	R	C_{29} 17aH, 21bH-Norhopane	65.121	19375	16.72	98
25	S	C_{29} 18aH-Norneohopane (29Ts)	65.347	5390	4.65	27
26	T	C_{30} 17aH Diahopane		0	0.00	<1
27	U	C_{29} 17bH, 21aH-Normoretane	67.108	3683	3.18	19
28	V	C_{30} 18aH+18bH-Oleanane		0	0.00	<1
29	W	C_{30} 17aH, 21bH-Hopane	68.573	19346	16.70	98
30	X	C_{30} 30-Nor-29-homo-17aH-hopane		0	0.00	<1
31	Y	C_{30} 17bH, 21aH-Moretane	70.107	8667	7.48	44
32	Z	C_{33} Tricyclic Terpane (22R)		0	0.00	<1
33	Z	C_{33} Tricyclic Terpane (22S)		0	0.00	<1
34	a	C_{31} 17aH, 21bH-Homohopane (22S)	72.583	8023	6.92	40
35	b	C_{31} 17aH, 21bH-Homohopane (22R)	73.071	11072	9.55	56
36	c	C_{30} Gammacerane	73.577	2807	2.42	14
37	d	C_{34} Tricyclic Terpane (22R)		0	0.00	<1
38	d	C_{34} Tricyclic Terpane (22S)		0	0.00	<1
39	e	C_{32} 17aH,21bH-Bishomohopane (22S)	75.791	4656	4.02	23
40	f	C_{32} 17aH, 21bH-Bishomohopane (22R)	76.488	5859	5.06	30
41	g	C_{35} Tricyclic Terpane (22R)		0	0.00	<1
42	g	C_{35} Tricyclic Terpane (22S)		0	0.00	<1
43	h	C_{33} 17aH, 21bH-Trishomohopane (22S)	79.505	3397	2.93	17
44	i	C_{33} 17aH, 21bH-Trishomohopane (22R)	80.446	3147	2.72	16
45	j	C_{34} 17aH, 21bH-Tetrahomohopane (22S)	83.340	2620	2.26	13
46	k	C_{34} 17aH, 21bH-Tetrahomohopane (22R)	84.508	3056	2.64	15
47	l	C_{35} 17aH, 21bH-Pentahomohopane (22S)	87.054	2378	2.05	12
48	m	C_{35} 17aH, 21bH-Pentahomohopane (22R)	88.362	1845	1.59	9

References

Avramidis, P., Zelilidis, A., Vakalas, I., Kontopoulos, N., 2002. Interactions between tectonic activity and eustatic sea-level changes in the Pindos and Mesohellenic basins, NW Greece: Basin evolution and hydrocarbon potential. J. Pet. Geol. 25, 53–82.

Brooks, J., Cornford, C., Archer, R., 1992. The role of hydrocarbon source rocks in petroleum exploration. In: Brooks, J., Fleet, A.J. (Eds.), Marine Petroleum Source Rocks. Spec. Publ. Geol. Soc., vol. 26, pp. 17–46.

Castaňo, J.R., Sparks, D.M., 1974. Interpretation of vitrinite reflectance measurements in sedimentary rocks and determination of burial history using vitrinite reflectance and authigenic minerals. Geol. Soc. Am., Spec. Pap. 153, 31–52.

Doutsos, T., Koukouvelas, I., Zelilidis, A., Kontopoulos, N., 1994. Intracontinental wedging and post-orogenic collapse in Mesohellenic Trough. Geol. Rundsch. 83, 257–275.

Dydik, B.M., Simoneit, B.R.T., Brassel, S.C., Eglinton, G., 1978. Organic geochemical indicators of palaeonvironmental conditions of sedimentation. Nature 272, 216–222.

Espitalié, J., La Porte, J.L, Madec, J., Marquis, F., Le Plat, P., Paulet, J., Boutefeu, A., 1977. Méthode rapide de charactérisation des roches mères de leur potentiel pétrolier et de leur degré d' évolution. Rev. Inst. Fr. Pet. 32, 23–42.

Ferriere, J., Reynaud, J., Pavlopoulos, A., Bonneau, M., Migiros, G., Chanier, F., Proust, J., Gardin, S., 2004. Geologic evolution and geodynamic controls of the Tertiary intramontane piggy-back Meso-hellenic basin, Greece. Bull. Soc. Geol. Fr. 175, 361–381.

Gerolymatos, H., Jacobshagen, P., Vasiliou, P., 1988. Geothermal evolution of Mesohellenic basin and organic matter maturation. Bull. Geol. Soc. Greece XX/2, 363–377.

Huang, W.Y., Meinschein, W.G., 1978. Sterols in sediments from Baffin Bay Texas. Geochim. Cosmochim. Acta 42, 1391.

Hunt, J., 1996. Petroleum Geochemistry and Geology. Freeman, San Francisco.

Killops, D., Killops, J., 1993. An introduction to organic geochemistry. Longman Sc. Tech.

Kontopoulos, N., Fokianou, T., Zelilidis, A., Alexiadis, C., Rigakis, N., 1999. Hydrocarbon potential of the middle Eocene–middle Miocene Mesohellenic piggy-back basin (Central Greece): a case study. Mar. Pet. Geol. 16, 811–824.

Leythaeuser, D., Schwarzkopf, T., 1986. The pristane/n-heptadecane ratio as an indicator for recognition of hydrocarbon migration effects. Org. Geochem. 10, 191–197.

Lo, H.B., 1993. Correction criteria for the suppression of vitrinite reflectance in hydrogen-rich kerogens: preliminary guidelines. Org. Geochem. 20, 653.

MacKenzie, A.S., Brassell, S.C., Eglinton, G., Maxwell, J.R., 1982. Chemical fossils, the geological fate of steroids. Science 217, 491–504.

Mavromatidis, A., Kelessidis, V.C., Monopolis, D.G., 2004. A review of recent hydrocarbon exploration and its potential. 1st Conference on Advances Mineral Resources Management Geotechnology, 7–9 June, pp. 1–8.

Moldowan, J.M., Seifert, W.K., Gallegos, E.J., 1985. Relationship between petroleum composition and depositional environment of petroleum source rocks. Am. Assoc. Pet. Geol. Bull. 69, 1255–1268.

Peters, K.E., 1986. Guidelines for evaluating petroleum source rock using programmed pyrolysis. Am. Assoc. Pet. Geol. Bull. 70, 318–329.

Peters, K.E., Moldowan, J.M., 1993. The Biomarker Guide: Interpreting Molecular Fossils in Petroleum and Ancient Sediments. Prenctile-Hall, Englewood Cliffs, NJ.

Potter, J.P., Stasiuk, L.D., Cameron, A.R., 1998. A petrographic atlas of Canadian coal macerals and dispersed organic matter.C.S.C.O. P.-G.S.C.-C.E.T.C., pp105.

Robertson, A.H.F., 1994. Role of the tectonic facies concept on orogenic analysis and its application to Tethys in the Eastern Mediterranean region. Earth-Sci. Rev. 24, 383–428.

Roussos, N., Marnelis, F., 1995. Greece licensing round to focus on western sedimentary basins. Oil Gas J. 93, 58–62.

Stach, E., Mackowsky, M., Teichmüller, M., Taylor, G., Chandra, D., Teichmüller, R., 1982. Stach's Textbook of Coal Petrology. Gebrüder Borntraeger, Berlin.

Staplin, F.L., 1969. Sedimentary organic matter, organic metamorphism and oil and gas occurrence. Bull. Can. Pet. Geol. 17, 47–66.

Stoykova, K., Avramidis, P., Zelilidis, A., 2002. Calcareous nannofossil stratigraphy of the Mesohellenic piggy-back basin, Central Greece. 9th International Nannoplankton Association Conference in Parma, Italy. Journal of Nannoplankton Research, vol. 24, p. 2.

Teichmueller, M., 1986. Organic petrology of source rocks history and state of the art. In: Leythaeuser, D., Rulkoetter, J. (Eds.), Advances in Organic Geochemistry, vol. 10, pp. 581–599.

Tissot, B.P., Welte, D.H., 1984. Petroleum Formation and Occurrence, second ed. Springer-Verlag.

van Krevelen, D.W., 1984. Organic geochemistry old and new. Org. Geochem. 6, 1–10.

Waples, D.W., 1980. Time and temperature in petroleum formation: application of Lopatin's method to petroleum exploration. Am. Assoc. Pet. Geol. Bull. 64, 916–926.

Zelilidis, A., Kontopoulos, N., Avramidis, P., Bouzos, D., 1997. Late Eocene to early Miocene depositional environments of the Mesohellenic basin, north-central Greece: implications for hydrocarbon potential. Geol. Balc. 27, 45–55.

Zelilidis, A., Piper, D.J.W., Kontopoulos, N., 2002. Sedimentation and basin evolution of the Oligocene–Miocene Mesohellenic basin, Greece. Am. Assoc. Pet. Geol. Bull. 86, 161–182.